Combined Role of the MJO and ENSO in Shaping Extreme Warming Patterns and Coral Bleaching Risk in the Great Barrier Reef

Catherine. H. Gregory[1,2], Neil. J. Holbrook[1,2,3], Andrew. G. Marshall[2,4,5], and Claire. M. Spillman[2,6]

[1] Institute for Marine and Antarctic Studies, University of Tasmania, Hobart, Tasmania, Australia.

[2]Australian Research Council Centre of Excellence for Climate Extremes, University of Tasmania, Hobart, Tasmania, Australia.

[3]Australian Research Council Centre of Excellence for the Weather of the 21st Century, University of Tasmania, Hobart, Tasmania, Australia.

[4] University of Southern Queensland, Toowoomba, Queensland, Australia.

[5] Bureau of Meteorology, Hobart, Tasmania, Australia.

[6] Bureau of Meteorology, Melbourne, Victoria, Australia.

Corresponding author: Catherine Gregory (catherine.gregory@utas.edu.au)

Key Points:

- Composite maps show how the Madden-Julian oscillation (MJO) can change meteorological patterns on the Great Barrier Reef.
- Cluster analysis is used to show types of MJO propagation patterns likely to occur during El Niño and La Niña periods.
- Ocean temperature variability is discussed with ENSO as the background driver and the MJO as a sub-seasonal modulator.

Abstract

Local meteorology over the Great Barrier Reef (GBR) can significantly influence ocean temperatures, which in turn impacts coral ecosystems. While El Niño–Southern Oscillation (ENSO) provides insight into the expected synoptic states, it lacks details of the anticipated sub-seasonal weather variability at local scales. This study explores the influence of the Madden-Julian oscillation (MJO) on Australian tropical climate, both independently and in combination with ENSO, with a focus on impacts to the GBR. We find that during El Niño periods, a faster propagating MJO pattern can disrupt background warm, dry conditions, and potentially provide cooling relief via increased cloud cover and stronger winds. Conversely, in La Niña periods, the MJO is prevented from passing the Maritime continent, forcing it to remain in a standing pattern in the Indian Ocean. This leads to reduced atmospheric convection over the GBR, decreased cloud cover and wind, and the generation of a warm ocean anomaly.

Plain Language Summary

Bleaching is likely when tropical corals are exposed to ocean temperatures above a threshold for a prolonged period. In austral summer, tropical weather over the Great Barrier Reef (GBR) can vary from hot and sunny to stormy with rain and strong winds. During El Niño, summer weather over the GBR is typically warm, still, and dry, increasing the likelihood of coral bleaching due to increased exposure to solar radiation and decreased mixing. During La Niña, tropical storms, with cooling effects through increased rainfall and cloud cover, are more typical. The Madden-Julian oscillation (MJO) is an eastward moving storm pattern near the equator that can also influence the background climate over the GBR. We find that the MJO can significantly influence the weather variability over the GBR during El Niño and La Niña periods.

1 Introduction

The Great Barrier Reef (GBR), located along Australia's northeast shelf, is the world's largest coral ecosystem, extending more than 2300km and consisting of almost 3000 individual reefs. It is renowned for its biodiversity, cultural significance (Marshall et al., 2019), and economic value, contributing around AU$6.4 billion annually to the Australian economy (O'Mahoney et al., 2017). However, corals have been seriously threatened in recent times with significant coral bleaching events (Hughes et al., 2017; McGowan and Theobald, 2023). Mass coral bleaching, due to prolonged, abnormally high ocean temperatures associated with climate change, is seen as the greatest threat to coral ecosystems (Ainsworth et al., 2016; Smith and Spillman, 2019; McWhorter et al., 2022). Although corals can recover from bleaching, the ongoing stress from rising ocean temperatures and other concurrent threats, such as ocean acidification and pollution, amplifies the risk of harm to the GBR (De'ath et al., 2012).

Sustained periods of sunny, weak wind days during the summer months can significantly increase the risk of coral bleaching, with reduced cloud cover leading to shallow water warming (Zhao et al., 2021) and low wind speeds reducing mixing (Bainbridge, 2017; Burt et al., 2019). The 2002 coral bleaching event in the GBR, for example, was attributed to anomalously low wind speeds and low evaporation rates which led to an accumulation of ocean heat (Liu et al., 2006). Conversely, coral bleaching risk tends to be reduced during periods of storms or high rainfall, as increased cloud cover can act to decrease sea surface temperatures (Hughes et al., 2017; Zhao et al., 2021) and strong winds increases evaporative cooling and mixing of warmer surface waters with cooler deep waters (MacKellar and McGowan, 2010; Yee and Barron, 2010). The passage of tropical cyclones can also reduce ocean temperatures across broad spatial scales, potentially mitigating mass coral bleaching events (Carrigan and Puotinen, 2014), although they may instead cause physical damage to coral reefs (Harmelin-Vivien, 1994; Dixon et al., 2022). Therefore, understanding the drivers of atmospheric variability over the GBR can inform potential predictability of bleaching events, which is essential for effective coral reef conservation and management (Smith and Spillman, 2019).

El Niño-Southern Oscillation (ENSO) is one of the primary drivers influencing the climate of the GBR region (Lough, 2007; Redondo-Rodriguez et al., 2011) with its peak phase aligning with the austral summer (December, January, February), when coral are most at risk of bleaching (Spillman and Alves, 2009). Extreme El Niño events, for example, were the leading drivers of the mass bleaching events in the GBR that occurred in 1983, 1998 and 2016 (Hughes et al., 2017). ENSO drives ocean temperature variability in this region indirectly through the local meteorology established by ocean-atmosphere

feedbacks (McGowan and Theobald, 2017), as shown in Figure 1. During El Niño events, sea surface temperatures (SSTs) are generally lower in the western Pacific Ocean during the early summer, reducing evaporation rates and resulting in reduced rainfall, a weaker monsoon, and high-pressure systems, often leading to increased surface ocean temperatures during the late summer months (Min et al., 2013; Gillett et al., 2023). Lower wind speeds in high-pressure systems often produce clearer waters due to less mixing and, combined with a lack of cloud cover, renders the coral more susceptible to damage through direct sunlight (UV) exposure (Fordyce et al., 2019).

On the other hand, SST anomalies during the austral spring months (September, October, November) of La Niña periods are generally positive in the GBR. These increased ocean temperatures result in the promotion of tropical storms, including tropical cyclones, that can prevent the accumulation of heat through increased shading and mixing between the warm upper and cool lower layers of the ocean. While these storm conditions may reduce the threat of extreme warming, it is important to note that they are often responsible for physical damage to coral reefs (Harmelin-Vivien, 1994; Osborne et al., 2011). Enhanced mixing, due to stronger winds, can also lead to more turbid conditions which, when combined with increased cloud cover, reduces the risk of damage from direct solar radiation (Fordyce et al., 2019). However, this does mean that the area is preconditioned to extreme warming if other factors restrict the formation of such storm patterns. While these climatic patterns of atmospheric variability due to ENSO are generally predictable on seasonal timescales, the instability of tropical weather often alters these patterns on sub-seasonal timescales.

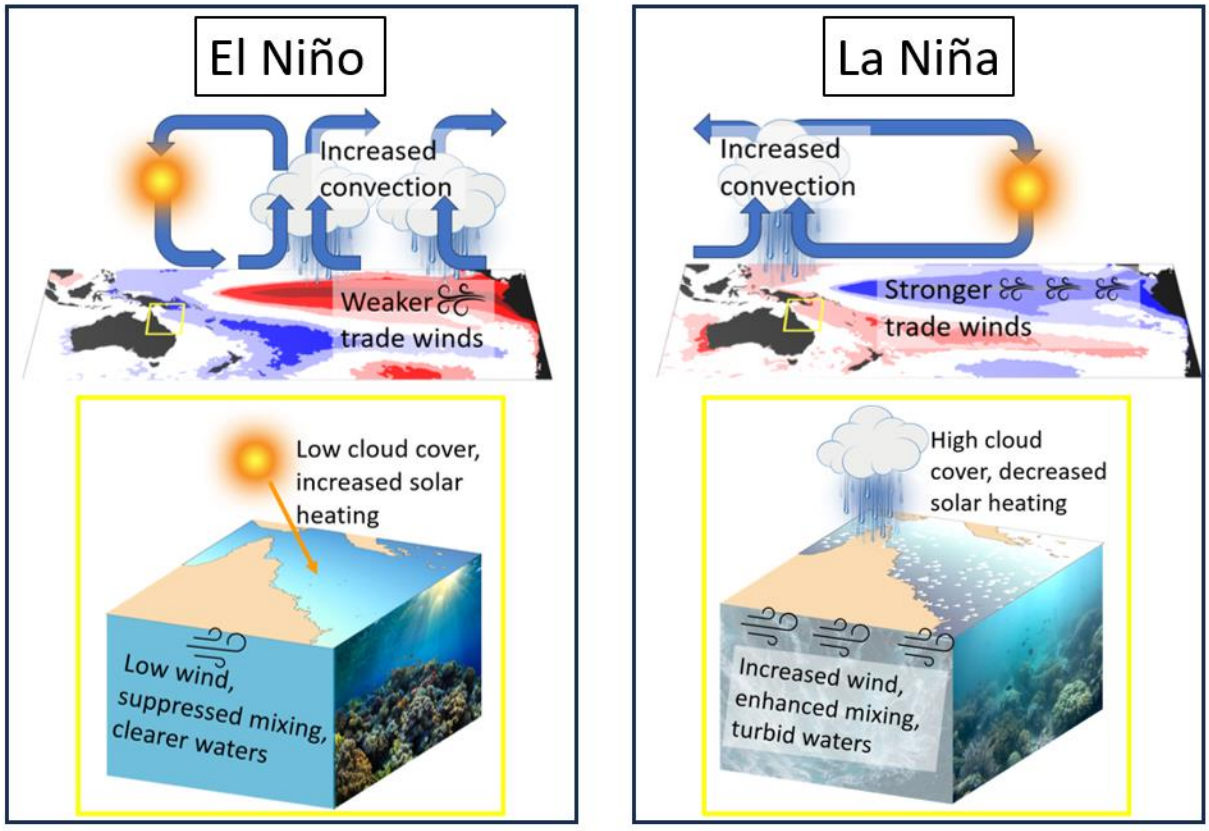

Figure 1
Schematics showing the large-scale ocean-atmosphere feedback processes that occur during El Niño and La Niña in the Pacific Ocean (blue indicates cool SST anomalies while red indicates warm SST anomalies), and the influence on local weather patterns over the GBR that contribute to significant ocean temperature variability and coral exposure to solar radiation.

The Madden-Julian oscillation (MJO) is the leading driver of sub-seasonal atmospheric variability in the tropics (Madden and Julian, 1994). Presenting as a slow, eastward moving storm pattern, the MJO propagates along the equator over a period of 30-90 days on average (Madden and Julian, 1971; Zhang, 2005). The MJO and ENSO are connected (Hoell et al., 2014), with seasonal MJO activity seen to precede ENSO related SST anomalies by several months (Zhang and Gottschalck, 2002). There is potential for the MJO to promote the onset of an El Niño by contributing to the buildup of warm water in the central equatorial Pacific This can be driven by zonal temperature advection through Kelvin waves (Hendon et al., 1998), or through the migration of convective energy (Bergman et al., 2001). ENSO has also been shown to impact the longitudinal extent of the MJO, causing an eastward shift during the mature phase of El Niño (Hendon et al., 1999; Kessler, 2001). However, the relationship is seasonally dependent (Hendon et al., 2007) and non-linear in nature (McPhaden et al., 2006). Therefore, assessing the interplay between ENSO, which provides the seasonal background context, and the MJO, capable of

modifying this background state, is crucial for understanding potential summertime weather and climate over the GBR.

In this paper, we investigate the relationship between ENSO and the MJO. We explore their individual and combined influences on atmospheric properties that act to increase or decrease ocean temperatures in the GBR, and that plays a role in enhancing or suppressing coral bleaching risk. By considering the most common types of MJO propagation patterns during El Niño and La Niña phases, we have uncovered an interesting negative feedback loop which can result in weather variations contrary to what would be expected by considering the influence of ENSO alone.

2 Data and Methods

2.1 Data

To calculate the atmosphere-ocean heat fluxes in the GBR region, we used daily output from the Bluelink ReANalysis (BRAN) 2020 (Chamberlain et al., 2021). This reanalysis dataset is produced by assimilating ocean observations into an eddy-resolving, near-global ocean circulation model, the Ocean Forecasting Australia Model (OFAM) v3 (Oke et al., 2013). This model is forced by atmospheric fluxes from the Japanese Meteorological Agency 55-year reanalysis (JRA-55) (Kobayashi et al., 2015).

We used outgoing longwave radiation (OLR) data from the U.S. National Oceanic and Atmospheric Administration (NOAA) OLR dataset estimated from polar-orbiting satellites and interpolated to include global spatial coverage on a daily timescale (Liebmann and Smith, 1996). The zonal and meridional wind fields used to show anomalous wind patterns in the MJO phases were taken from the National Center for Environmental Prediction/National Center for Atmospheric Research (NCEP/NCAR) Reanalysis 2 product. These data were generated using a forecast model that assimilates observational data (Kanamitsu et al., 2002) and, with a relatively coarse spatial grid of 2.5 degrees, is well suited for the analysis of large scale processes (Dufek et al., 2008).

Finally, SST data used to show the background state of the ocean during different MJO types (typological classes) were from the NOAA Optimum Interpolation Sea Surface Temperature V2.1 (OISSTv2.1) dataset. These 0.25° gridded global SST data are from high-resolution infrared and microwave satellites blended with in-situ observational data from ships and buoys, and comprise daily SSTs from 1982 to the present day (Reynolds et al., 2007; Banzon et al., 2016; Huang et al., 2021).

2.2 Calculation of indices

The MJO index was calculated using the Real-time Multivariate MJO (RMM) method of Wheeler and Hendon (2004), where the principal component time series of the leading pair of empirical orthogonal functions from averaged fields of the 200 hPa and 850 hPa zonal winds and OLR near the equator are

used to describe the strength (amplitude) and position (phase) of the MJO along the equator. We consider the MJO to be in phase when the amplitude is >1.

NOAA's Oceanic Niño Index (ONI) (Bamston et al., 1997) was used to indicate the phase of ENSO. An El Niño state was defined when SST anomalies in the Niño 3.4 region (5°S – 5°N, 170°W-120°W) exceeded +0.5°C for five consecutive months, using a three-month running mean. Conversely, a La Niña state was identified when SST anomalies fell below -0.5°C for that region for the same consecutive period.

2.3 Heat flux anomalies

The additional heat entering the ocean due to positive heat fluxes during each of the phases of the MJO was calculated by summing the net contributions from the shortwave (solar) radiation, longwave (thermal) radiation, sensible heat exchange due to the difference between atmospheric and oceanic temperature, and latent heat due to evaporation such that:

$$Q_{net} = Q_{SW} + Q_{LW} + Q_{Sen} + Q_{Lat} \quad (1)$$

and scaling by the seawater density (ρ), heat capacity (C_p) and mixed layer depth (H).

$$\text{Heat flux} = \frac{Q_{net}}{\rho C_p H} \quad (2)$$

Note that we ignore the effects of upper ocean advection in this basic heat flux calculation, which we deem to play a much smaller role in the local heating response.

2.4 Diversity of MJO events

To group individual MJO events by their propagation patterns, we used a modified version of the method employed by Wang et al. (2019). Following their study, we defined a MJO event during the extended austral summer (from November to April for 1982-2023) when the 20- to 70-day band-pass–filtered OLR anomalies in the eastern Indian Ocean region (10°S to 10°N and 75°E to 95°E) were less than one standard deviation for at least five consecutive days. To identify the different propagation patterns of these events, a ***k***-means cluster analysis (Forgy, 1965) was performed on the latitudinally-averaged Hovmöller plots of each of the events. The plots covered a longitudinal extent of 60°E to 180°E from 10 days before to 20 days after the start day of each event, to consider its propagation from the Indian Ocean eastward beyond Australia. Each of the events was assigned to one of the leading four nodes (Supplementary Fig. 1). Of the 120 individual events detected, the patterns of 11 events did not

sufficiently match any of the centroids of the clusters. For more information on this methodology, see Wang et al. (2019).

3 Results

3.1 Influence of the MJO

The influence of the MJO on weather patterns in the GBR region and resulting heat flux changes, during the extended austral summer (November to April), are shown in Figure 2. When the winds converge in the Indian Ocean to develop the storm pattern in MJO phases 2-3, the GBR region experiences clearer skies (Fig 2.a), and lower wind speeds (Fig 2.e), resulting in a positive heat flux into the ocean (Fig. 2i). As this storm pattern moves over the maritime continent in MJO phases 4-5, the cloud cover begins to increase in the GBR region (Fig. 2b), reducing the amount of heat entering the ocean (Fig. 2j). As the MJO passes the Australian continent and moves across the Pacific Ocean in MJO phases 6-7, the cloud cover is at its maximum over the GBR region (Fig. 2c) and wind speeds increase (Fig. 2g), resulting in heat loss in the northern GBR (Fig. 2k). Finally, as the MJO continues to move across the Pacific Ocean in MJO phases 8-1, the patterns of reduced cloud (Fig. 2d) and reduced wind speeds (Fig. 2h) result in a positive heat flux in the northern GBR region (Fig. 2l).

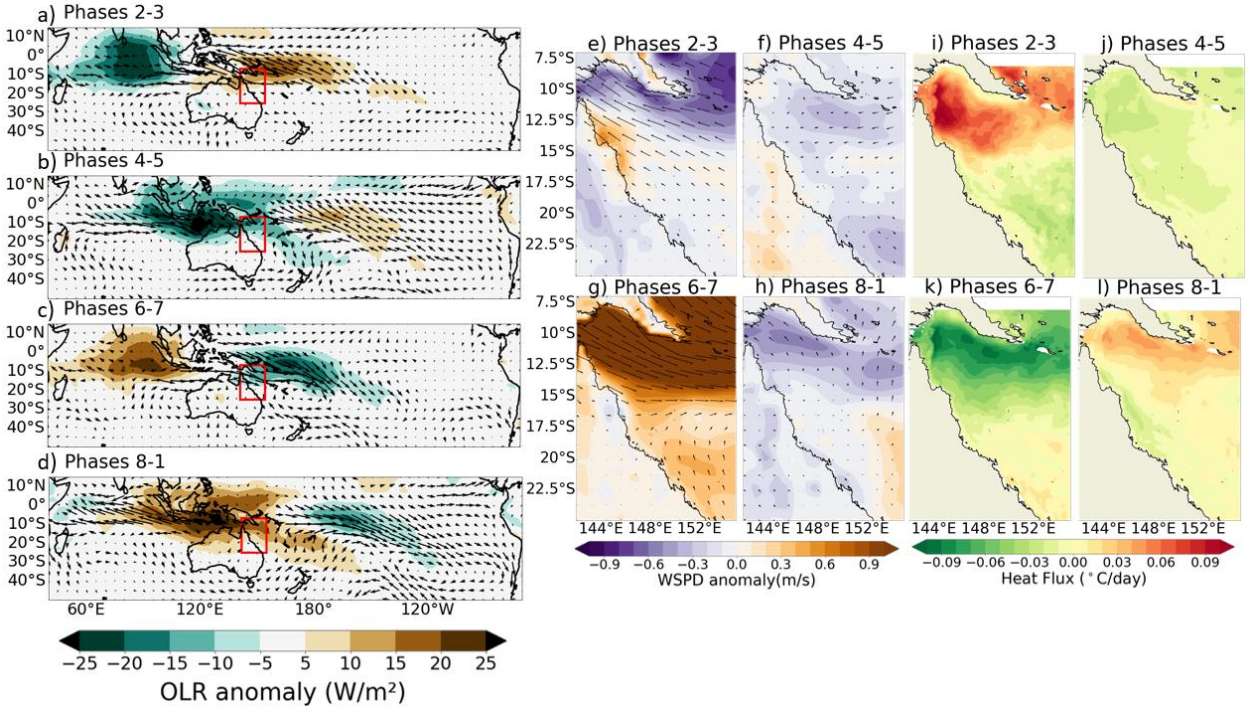

Figure 2

Composite maps for the extended austral summer (from November to April) during the phase pairs of the MJO, together with their impact on the heat fluxes into the ocean in the GBR region. (a-d) OLR (shading) and wind direction (vectors) anomalies, (e-h) local wind speed anomalies (shading), wind direction (vectors) and (i-l) heat flux

anomalies, where positive values represent an increase of heat into the ocean. All composites were created using data from 1993-2023.

3.2 The MJO and ENSO

Using the *k*-means cluster analysis, we grouped 109 individual MJO events into four categories – standing, jumping, fast propagating and slow propagating, as in Wang et al. (2019). As we are interested in the connection between ENSO and the MJO, we focused on the standing and fast propagating categories as they are associated with ENSO phases, while the analysis of all four categories can be found in the supplementary information (Supplementary Fig. 2). Figure 3 shows the evolution of OLR anomalies (negative shown as dashed contours, positive shown as solid contours) and the background SST anomalies (shading) during the standing and fast propagating MJO types, as composites of 5-day groupings from 10 days before until 20 days after the start date of each event. The left column shows the standing pattern connected to the La Niña phase. Prior to the commencement of the MJO events, there is a region of positive OLR anomalies in the western Pacific Ocean (Fig 3a). As the convective energy starts to build in the Indian Ocean from five days prior (Fig 3.c) to 5 days after (Fig 3.e) the start date, the region of positive OLR anomalies to the east of the Australia is drawn across the north of the continent. During the first 20 days, the MJO fails to move past the Maritime Continent and remains in the Indian Ocean, characteristic of its early phases.

The right column shows the fast propagation pattern connected with El Niño. From 10 days prior to the start of these events until five days after, there is a notable pattern of positive OLR anomalies (i.e. reduced cloud cover) to the north of Australia, associated with the El Niño state (see Figure 1). The convective energy associated with the early phases of the MJO is seen to begin to build up in the Indian Ocean as early as 5 to 10 days before the official start of these events (Fig. 3b) and continues to increase until 5 to 10 days after the start day. At this point, the MJO can be seen to push through the positive OLR anomalies (Fig. 3h) until it reaches the Pacific Ocean, where it acts to extend the reach of the cloud cover (Fig 3.l).

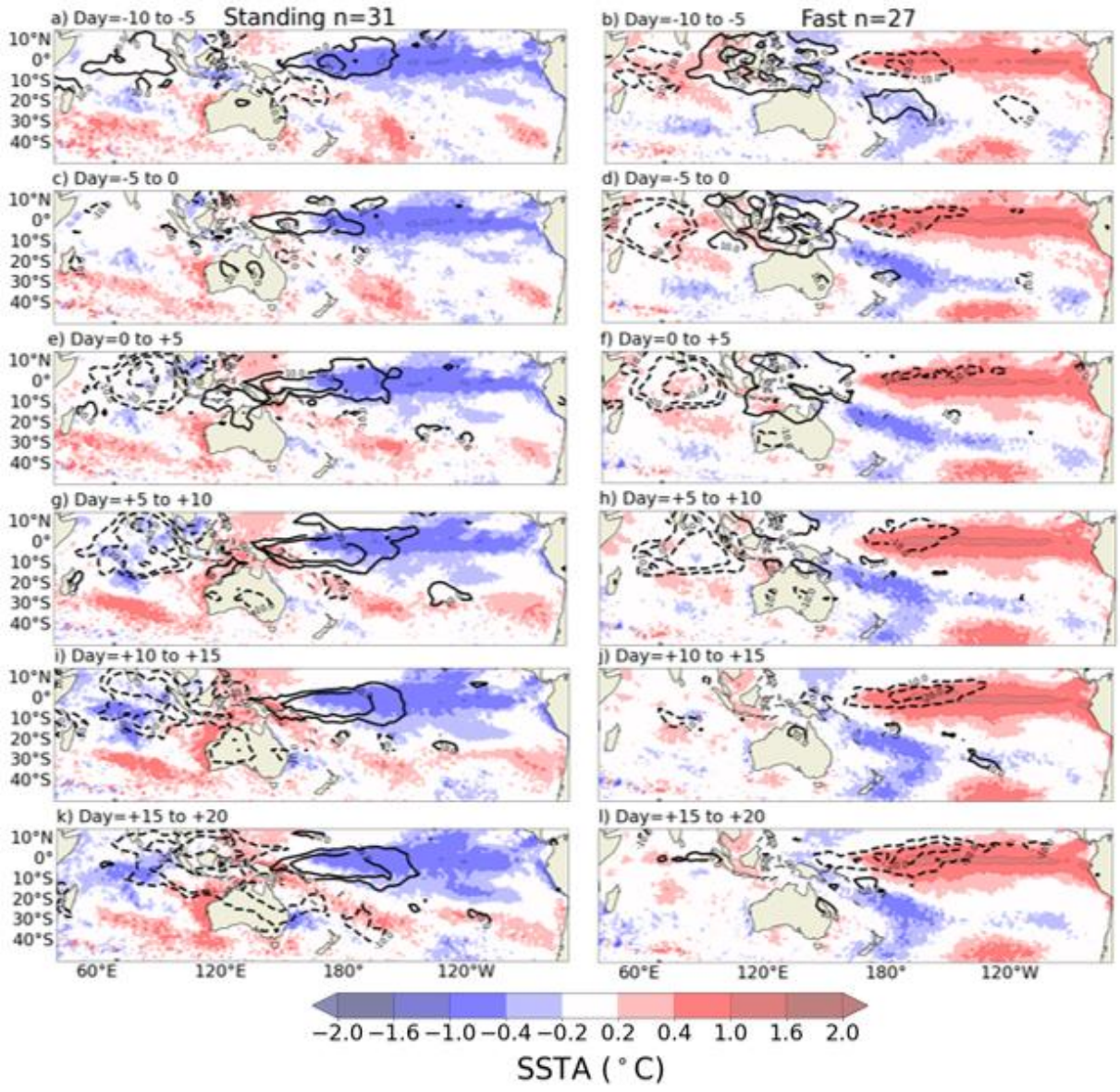

Figure 3

Composite maps of the propagation patterns (using 5-day windows) of two distinct typological classes of the MJO and associated SST anomalies, where day 0 is the start day of a MJO event. The convective centre representing the position of the MJO is shown by negative OLR anomalies (dashed contours). The standing pattern connected to La Niña is shown in the left column and the fast-propagating pattern connected to El Niño is shown in the right column. The *n*-values show the number of separate MJO events in each of these groups.

4 Summary

Figure 4 is a schematic representation of the individual and cumulative influence of ENSO and the MJO on the atmospheric states, resulting in changes to sea surface temperatures in the GBR region. The orange panels include the expected seasonal background states during El Niño and La Niña periods (Figure 4). El Niño phases are characterised by cooler SSTs in the western South Pacific Ocean that reduce evaporation rates and act to reduce cloud cover and form fewer and/or less intense storms. Over months, these conditions act to warm and further stratify the upper ocean. During La Niña, warmer ocean temperatures in the western South Pacific precondition the GBR region to warming. However, as warm, moist air rises from the ocean surface over the region, it cools and condenses aiding in the formation of deep convective clouds. This in turn leads to increased wind speeds and reduced solar radiation, cooling the surface ocean.

However, the MJO plays an important modulating role. During El Niño, warmer SSTs in the eastern Pacific and weaker easterly winds draw the MJO from the Indian Ocean across the maritime continent and into the Pacific Ocean into phases 5-6-7 (Fig. 3 right column). These later phases bring an increase in cloud cover and stronger winds (Fig. 2), and have been shown to be more favourable during this time to tropical cyclone genesis (Lee et al., 2018), often resulting in a cooling effect in the region. The opposite can be seen during La Niña periods, when the MJO is prevented from crossing the maritime continent, forcing it to remain in its early phases (Fig. 3 left). These phases lead to a reduction in cloud cover and weaker winds in the GBR and Coral Sea region (Fig. 2) and a reduction in tropical cyclone occurrences (Lee et al., 2018), which can act to further warm the region, already preconditioned to warming due to the La Niña phase.

A positive feedback loop can also be established during El Niño years, with the Indo-Pacific Warm Pool expanding and increasing the zonal scale of the MJO (Zhang, 2005), which contributes to westerly wind bursts (WWBs), and with stronger MJO events leading to more intense WWBs (Liang et al., 2021). These WWBs generate eastward surface currents at the equator and downwelling Kelvin waves that considerably increase the strength of the El Niño (Fedorov, 2002; Lian et al., 2014; Chen et al., 2015).

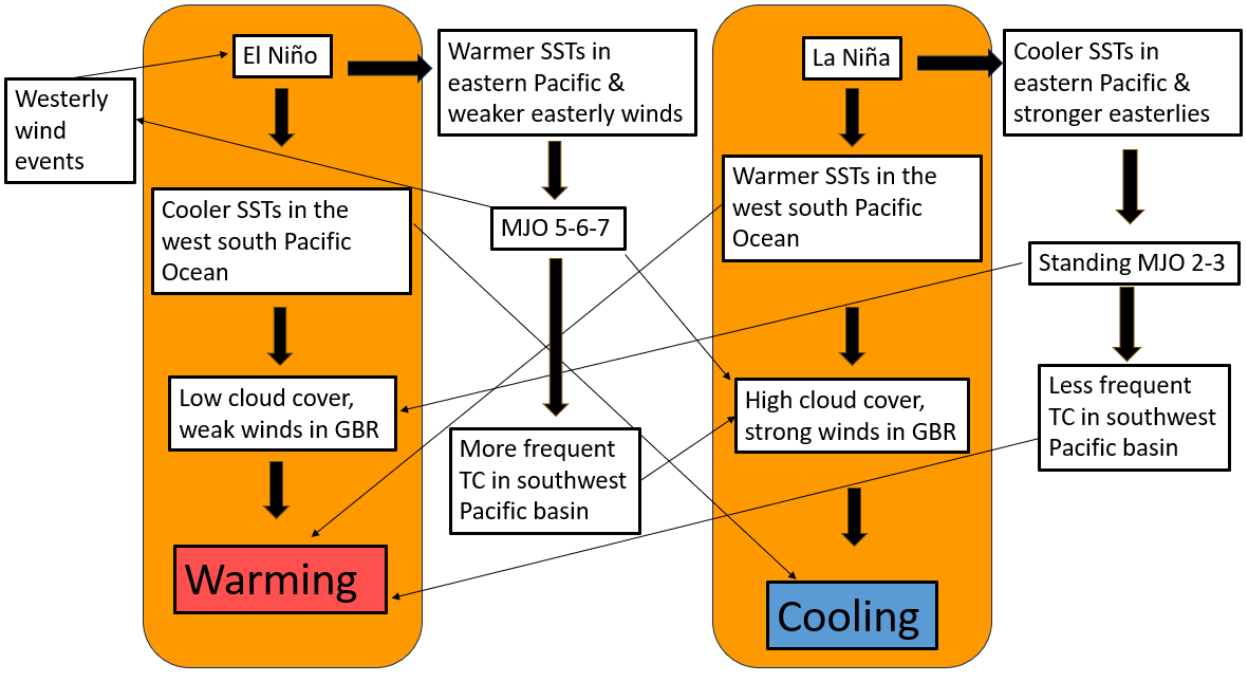

Figure 4

Schematic showing the complex interplay between the MJO and ENSO and the variety of paths that can be taken to eventually result in warming or cooling of the GBR region SSTs. The panels in orange represent the typical background conditions associated with the phases of ENSO (El Nino and La Nina), when MJO is weak or inactive. The boxes outside of the orange panels show how the background ENSO state can influence the propagation of the MJO, leading to changes in the atmospheric conditions over the GBR.

5 Discussion

In this study, we have shown how the MJO can dynamically shape weather patterns over the Great Barrier Reef (GBR) by modulating the synoptic conditions against the background ENSO phase. It has been previously highlighted that regional meteorology plays a significant role in influencing sea surface temperatures in the GBR region, and thus impacting coral health (e.g. (McGowan and Theobald, 2017; Karnauskas, 2020; McGowan and Theobald, 2023; Huang et al., 2024)**.** The vulnerability of reef systems in this region is most pronounced during the austral summer months due to peak ocean temperatures (Hoegh-Guldberg, 1999; Spillman and Alves, 2009). This also coincides with both the peak of the ENSO cycle (Philander, 1983) and the increased influence of the MJO in the region due to its position south of the equator during this time (Zangvil, 1975; Wheeler and Hendon, 2004).

We found that the atmospheric patterns linked to the phases of ENSO have the potential to evoke the types of MJO propagations that can lead to negative feedback loops. The fast-propagating MJO type can disrupt periods of reduced cloud cover in northern Australia (Fig. 3 right column) and draw the MJO into phases 6-7 associated with strong winds (Fig. 2g) and heat fluxes from the ocean to the atmosphere (Fig. 2k). During these times, coral reefs in the region experience a respite from the prevailing warm El Niño conditions (Fig. 1). This was seen during the 2015/16 extreme El Niño event where a very active MJO traversed northern Australia in December, halting the spring warming due to increased cloud cover and rainfall. However, the MJO remained active, advancing to the east Pacific Ocean in January and leading to suppressed convection over tropical Australia once again, exacerbating the warming effect (Benthuysen et al., 2018).

Conversely, under atmospheric conditions during La Niña, there is an observed inhibition of MJO propagation beyond the Maritime Continent (Fig. 3 left column). This standing MJO remains in the early phases (2-3), exposing the GBR to periods of reduced cloud cover and weaker winds (Fig. 2 a,e,i) – contrary to the anticipated typical La Niña conditions (Fig. 1). This phenomenon provides insight into the bleaching event witnessed in early 2022. While this event was linked to unusual weather patterns (e.g. McGowan and Theobald 2023), it was widely reported in the media that the main cause was increasing ocean temperatures due to climate change (Whiteman et al., 2022). However, during February and March of 2022, the MJO remained in phases 1-4 (Supplementary Fig. 2), likely aided by the La Niña conditions, which would explain the anomalous lack of clouds and wind which led to the bleaching event. While acknowledging that increased ocean temperatures due to climate change pose the primary long-term threat to coral reefs (Hoegh-Guldberg et al., 2007; Hughes et al., 2018; Sully et al., 2019), accurate attribution of the drivers of individual coral bleaching incidents is important for more effective shorter-term diagnoses, as well as management and planning (Trenberth et al., 2015).

There are several theories to explain the eastward propagation of the MJO, including the moisture mode theory (Sobel et al., 2014). From this perspective, the eastward propagation of the MJO convection is favoured when there is an increase in the moist static energy (MSE) to the east of the MJO (Hsu et al., 2014). During El Niño periods, the increased SSTs in the east equatorial Pacific results in a higher atmospheric moisture content which increases the MSE (Back and Bretherton, 2006). During these periods, the lower troposphere in the Pacific becomes destabilised (Wang et al., 2019), enhancing convection and the zonal length of the vertical overturning circulation, allowing the MJO to propagate further (Hu and Li, 2022).

Both the MJO and ENSO have also been seen to influence tropical cyclone activity. Tropical cyclones in the Australian region typically occur between November and April (Chand et al., 2019). El Niño periods are accompanied by reduced cyclone activity over the northeast Australian coast and a later start to the Australian monsoon season, generally beginning as El Niño declines in the late austral summer (Wang et al., 2003). Enhanced tropical cyclone activity is common in La Niña periods across northern Australia, assisted by elevated SSTs in the western Pacific Ocean (Hastings, 1990; Evans and Allan, 1992). MJO activity can influence the wind patterns influencing cyclogenesis (Hall et al., 2001), with stronger wind patterns in the western Pacific Ocean during MJO phases 5-6 favoring both the development and strength of cyclones in the Australian region, and weaker winds during MJO phases 2-3 hindering the development of cyclones in this region (Lee et al., 2018).

Correct attribution of extreme events is a complicated task (Trenberth et al., 2015). Contemporary discourse frequently emphasises the pivotal role of climate change in influencing extreme events, yet this tends to dismiss the roles of climate modes, which are also important drivers of these events. Although climate change undeniably serves as a crucial factor contributing to the heightened intensity and frequency of extreme events (Mitchell et al., 2006; Lee et al., 2023), it is essential to understand the thermodynamic drivers to more precisely comprehend the specific influence of climate change on the dynamics of extreme events. While increased ocean temperatures have heightened the general susceptibility of corals to bleaching (Hoegh-Guldberg, 2011), climate change is also anticipated to exert changes to the modes of climate variability, including ENSO (Cai et al., 2015). The expanding Indo-Pacific Warm Pool, for example, acts as a catalyst in reshaping atmospheric patterns that will see the MJO have an eastward longitudinal expansion and an overall acceleration in propagation speed (Cui and Li, 2019). By understanding the dynamic interactions between the MJO and ENSO and their impact on weather patterns in the GBR region there is potential to improve our forecasting capabilities. This will be of benefit to those marine resource managers who require accurate forecasts of summer conditions to make informed decisions to effectively preserve and protect the integrity of the GBR.

Acknowledgments

The authors declare that there are no known competing interests, whether personal, professional, or financial, that would influence the findings of this paper.

CHG was supported by an ARC Centre of Excellence for Climate Extremes (CLEX) PhD scholarship. CHG is also grateful for additional top-up support from the joint CSIRO-UTAS Quantitative Marine Science program and the Australian Bureau of Meteorology.
NJH acknowledges support from the ARC Centre of Excellence for Climate Extremes (CE170100023), the ARC Centre of Excellence for the Weather of the 21st Century (CE230100012), and the National Environmental Science Program Climate Systems Hub.
AGM and CMS would like to acknowledge support from the Australian Bureau of Meteorology.
We are grateful for the computational support from Australia's National Computational Infrastructure (NCI) and the CLEX Computational Modelling Support (CMS) team.

Data Availability Statement

All datasets used in this study are open-source and available to be downloaded online.
The OISST v2, NOAA OLR, and NCEP/NCAR datasets were provided by the NOAA/OAR/ESRL PSL, Boulder, Colorado, USA, via their website at https://psl.noaa.gov/
The BRAN202 dataset is publicly available at
https://dapds00.nci.org.au/thredds/catalog/gb6/BRAN/catalog.html

References

Ainsworth, T.D., Heron, S.F., Ortiz, J.C., Mumby, P.J., Grech, A., Ogawa, D., Eakin, C.M., and Leggat, W. (2016). Climate change disables coral bleaching protection on the Great Barrier Reef. *Science* 352**,** 338-342.

Back, L.E., and Bretherton, C.S. (2006). Geographic variability in the export of moist static energy and vertical motion profiles in the tropical Pacific. *Geophysical Research Letters* 33.

Bainbridge, S.J. (2017). Temperature and light patterns at four reefs along the Great Barrier Reef during the 2015–2016 austral summer: understanding patterns of observed coral bleaching. *Journal of Operational Oceanography* 10**,** 16-29.

Bamston, A.G., Chelliah, M., and Goldenberg, S.B. (1997). Documentation of a highly ENSO-related sst region in the equatorial pacific: Research note. *Atmosphere-Ocean* 35**,** 367-383.

Banzon, V., Smith, T.M., Chin, T.M., Liu, C., and Hankins, W. (2016). A long-term record of blended satellite and in situ sea-surface temperature for climate monitoring, modeling and environmental studies. *Earth System Science Data* 8**,** 165-176.

Benthuysen, J.A., Oliver, E.C.J., Feng, M., and Marshall, A.G. (2018). Extreme Marine Warming Across Tropical Australia During Austral Summer 2015–2016. *Journal of Geophysical Research: Oceans* 123**,** 1301-1326.

Bergman, J.W., Hendon, H.H., and Weickmann, K.M. (2001). Intraseasonal Air–Sea Interactions at the Onset of El Niño. *Journal of Climate* 14**,** 1702-1719.

Burt, J.A., Paparella, F., Al-Mansoori, N., Al-Mansoori, A., and Al-Jailani, H. (2019). Causes and consequences of the 2017 coral bleaching event in the southern Persian/Arabian Gulf. *Coral Reefs* 38**,** 567-589.

Cai, W., Santoso, A., Wang, G., Yeh, S.-W., An, S.-I., Cobb, K.M., Collins, M., Guilyardi, E., Jin, F.-F., and Kug, J.-S. (2015). ENSO and greenhouse warming. *Nature Climate Change* 5**,** 849-859.

Carrigan, A.D., and Puotinen, M. (2014). Tropical cyclone cooling combats region-wide coral bleaching. *Global Change Biology* 20**,** 1604-1613.

Chand, S.S., Dowdy, A.J., Ramsay, H.A., Walsh, K.J.E., Tory, K.J., Power, S.B., Bell, S.S., Lavender, S.L., Ye, H., and Kuleshov, Y. (2019). Review of tropical cyclones in the Australian region: Climatology, variability, predictability, and trends. *WIREs Climate Change* 10**,** e602.

Chen, D., Lian, T., Fu, C., Cane, M.A., Tang, Y., Murtugudde, R., Song, X., Wu, Q., and Zhou, L. (2015). Strong influence of westerly wind bursts on El Niño diversity. *Nature Geoscience* 8**,** 339-345.

Cui, J., and Li, T. (2019). Changes of MJO propagation characteristics under global warming. *Climate Dynamics* 53**,** 5311-5327.

De'ath, G., Fabricius, K., Sweatman, H., and Puotinen, M. (2012). "The 27-year decline of coral cover on the Great Barrier Reef and its causes, 1–5. Retrieved October 2, 2012".).

Dixon, A.M., Puotinen, M., Ramsay, H.A., and Beger, M. (2022). Coral reef exposure to damaging tropical cyclone waves in a warming climate. *Earth's Future* 10**,** e2021EF002600.

Dufek, A.S., Ambrizzi, T., and Da Rocha, R.P. (2008). Are Reanalysis Data Useful for Calculating Climate Indices over South America? *Annals of the New York Academy of Sciences* 1146**,** 87-104.

Evans, J.L., and Allan, R.J. (1992). El Niño/Southern Oscillation modification to the structure of the monsoon and tropical cyclone activity in the Australasian region. *International Journal of Climatology* 12**,** 611-623.

Fedorov, A.V. (2002). The response of the coupled tropical ocean–atmosphere to westerly wind bursts. *Quarterly Journal of the Royal Meteorological Society* 128**,** 1-23.

Fordyce, A.J., Ainsworth, T.D., Heron, S.F., and Leggat, W. (2019). Marine heatwave hotspots in coral reef environments: physical drivers, ecophysiological outcomes, and impact upon structural complexity. *Frontiers in Marine Science* 6**,** 498.

Forgy, E.W. (1965). Cluster analysis of multivariate data: efficiency versus interpretability of classifications. *biometrics* 21**,** 768-769.

Gillett, Z., Taschetto, A., Holgate, C., and Santoso, A. (2023). Linking ENSO to synoptic weather systems in Eastern Australia. *Geophysical Research Letters* 50**,** e2023GL104814.

Hall, J.D., Matthews, A.J., and Karoly, D.J. (2001). The Modulation of Tropical Cyclone Activity in the Australian Region by the Madden–Julian Oscillation. *Monthly Weather Review* 129**,** 2970-2982.

Harmelin-Vivien, M.L. (1994). The effects of storms and cyclones on coral reefs: a review. *Journal of Coastal Research***,** 211-231.

Hastings, P.A. (1990). Southern Oscillation influences on tropical cyclone activity in the Australian/south-west Pacific region. *International Journal of climatology* 10**,** 291-298.

Hendon, H.H., Liebmann, B., and Glick, J.D. (1998). Oceanic Kelvin Waves and the Madden–Julian Oscillation. *Journal of the Atmospheric Sciences* 55**,** 88-101.

Hendon, H.H., Wheeler, M.C., and Zhang, C. (2007). Seasonal dependence of the MJO–ENSO relationship. *Journal of climate* 20**,** 531-543.

Hendon, H.H., Zhang, C., and Glick, J.D. (1999). Interannual Variation of the Madden–Julian Oscillation during Austral Summer. *Journal of Climate* 12**,** 2538-2550.

Hoegh-Guldberg, O. (1999). Coral bleaching, climate change, and the future of the world's coral reefs. *Mar Freshw Res* 50**,** 839-866.

Hoegh-Guldberg, O. (2011). The impact of climate change on coral reef ecosystems. *Coral reefs: an ecosystem in transition***,** 391-403.

Hoegh-Guldberg, O., Mumby, P.J., Hooten, A.J., Steneck, R.S., Greenfield, P., Gomez, E., Harvell, C.D., Sale, P.F., Edwards, A.J., and Caldeira, K. (2007). Coral reefs under rapid climate change and ocean acidification. *science* 318**,** 1737-1742.

Hoell, A., Barlow, M., Wheeler, M.C., and Funk, C. (2014). Disruptions of El Niño–Southern Oscillation Teleconnections by the Madden–Julian Oscillation. *Geophysical Research Letters* 41**,** 998-1004.

Hsu, P.-C., Li, T., and Murakami, H. (2014). Moisture Asymmetry and MJO Eastward Propagation in an Aquaplanet General Circulation Model. *Journal of Climate* 27**,** 8747-8760.

Hu, F., and Li, T. (2022). Effect of vertical overturning circulation scale and moist static energy tendency on MJO phase speed. *Atmospheric and Oceanic Science Letters* 15**,** 100150.

Huang, B., Liu, C., Freeman, E., Graham, G., Smith, T., and Zhang, H.-M. (2021). Assessment and intercomparison of NOAA daily optimum interpolation sea surface temperature (DOISST) version 2.1. *Journal of Climate* 34**,** 7421-7441.

Huang, Z., Feng, M., Dalton, S.J., and Carroll, A.G. (2024). Marine heatwaves in the Great Barrier Reef and Coral Sea: their mechanisms and impacts on shallow and mesophotic coral ecosystems. *Science of The Total Environment* 908**,** 168063.

Hughes, T.P., Anderson, K.D., Connolly, S.R., Heron, S.F., Kerry, J.T., Lough, J.M., Baird, A.H., Baum, J.K., Berumen, M.L., and Bridge, T.C. (2018). Spatial and temporal patterns of mass bleaching of corals in the Anthropocene. *Science* 359**,** 80-83.

Hughes, T.P., Kerry, J.T., Álvarez-Noriega, M., Álvarez-Romero, J.G., Anderson, K.D., Baird, A.H., Babcock, R.C., Beger, M., Bellwood, D.R., Berkelmans, R., Bridge, T.C., Butler, I.R., Byrne, M., Cantin, N.E., Comeau, S., Connolly, S.R., Cumming, G.S., Dalton, S.J., Diaz-Pulido, G., Eakin, C.M., Figueira, W.F., Gilmour, J.P., Harrison, H.B., Heron, S.F., Hoey, A.S., Hobbs, J.-P.A., Hoogenboom, M.O., Kennedy, E.V., Kuo, C.-Y., Lough, J.M., Lowe, R.J., Liu, G., Mcculloch, M.T., Malcolm, H.A., Mcwilliam, M.J., Pandolfi, J.M., Pears, R.J., Pratchett, M.S., Schoepf, V., Simpson, T., Skirving, W.J., Sommer, B., Torda, G., Wachenfeld, D.R., Willis, B.L., and Wilson, S.K. (2017). Global warming and recurrent mass bleaching of corals. *Nature* 543**,** 373-377.

Kanamitsu, M., Ebisuzaki, W., Woollen, J., Yang, S.-K., Hnilo, J.J., Fiorino, M., and Potter, G.L. (2002). NCEP–DOE AMIP-II Reanalysis (R-2). *Bulletin of the American Meteorological Society* 83**,** 1631-1644.

Karnauskas, K.B. (2020). Physical Diagnosis of the 2016 Great Barrier Reef Bleaching Event. *Geophysical Research Letters* 47**,** e2019GL086177.

Kessler, W.S. (2001). EOF Representations of the Madden–Julian Oscillation and Its Connection with ENSO. *Journal of Climate* 14**,** 3055-3061.

Kobayashi, S., Ota, Y., Harada, Y., Ebita, A., Moriya, M., Onoda, H., Onogi, K., Kamahori, H., Kobayashi, C., and Endo, H. (2015). The JRA-55 reanalysis: General specifications and basic characteristics. *Journal of the Meteorological Society of Japan. Ser. II* 93**,** 5-48.

Lee, C.-Y., Camargo, S.J., Vitart, F., Sobel, A.H., and Tippett, M.K. (2018). Subseasonal Tropical Cyclone Genesis Prediction and MJO in the S2S Dataset. *Weather and Forecasting* 33**,** 967-988.

Lee, H., Calvin, K., Dasgupta, D., Krinmer, G., Mukherji, A., Thorne, P., Trisos, C., Romero, J., Aldunce, P., and Barret, K. (2023). Synthesis report of the IPCC Sixth Assessment Report (AR6), Longer report. IPCC.

Lian, T., Chen, D., Tang, Y., and Wu, Q. (2014). Effects of westerly wind bursts on El Niño: A new perspective. *Geophysical Research Letters* 41**,** 3522-3527.

Liang, Y., Fedorov, A.V., and Haertel, P. (2021). Intensification of Westerly Wind Bursts Caused by the Coupling of the Madden-Julian Oscillation to SST During El Niño Onset and Development. *Geophysical Research Letters* 48**,** e2020GL089395.

Liebmann, B., and Smith, C.A. (1996). Description of a complete (interpolated) outgoing longwave radiation dataset. *Bulletin of the American Meteorological Society* 77**,** 1275-1277.

Liu, G., Strong, A.E., Skirving, W., and Arzayus, L.F. (Year). "Overview of NOAA coral reef watch program's near-real time satellite global coral bleaching monitoring activities", in: *Proceedings of the 10th international coral reef symposium*: Gurugram Okinawa, Japan), 1783-1793.

Lough, J. (2007). Climate and climate change on the Great Barrier Reef.

Mackellar, M.C., and Mcgowan, H.A. (2010). Air-sea energy exchanges measured by eddy covariance during a localised coral bleaching event, Heron Reef, Great Barrier Reef, Australia. *Geophysical Research Letters* 37.

Madden, R.A., and Julian, P.R. (1971). Detection of a 40–50 day oscillation in the zonal wind in the tropical Pacific. *Journal of Atmospheric Sciences* 28**,** 702-708.

Madden, R.A., and Julian, P.R. (1994). Observations of the 40–50-day tropical oscillation—A review. *Monthly weather review* 122**,** 814-837.

Marshall, N., Adger, W.N., Benham, C., Brown, K., I Curnock, M., Gurney, G.G., Marshall, P., L Pert, P., and Thiault, L. (2019). Reef Grief: investigating the relationship between place meanings and place change on the Great Barrier Reef, Australia. *Sustainability Science* 14**,** 579-587.

Mcgowan, H., and Theobald, A. (2017). ENSO Weather and Coral Bleaching on the Great Barrier Reef, Australia. *Geophysical Research Letters* 44**,** 10,601-610,607.

Mcgowan, H., and Theobald, A. (2023). Atypical weather patterns cause coral bleaching on the Great Barrier Reef, Australia during the 2021–2022 La Niña. *Scientific Reports* 13**,** 6397.

Mcphaden, M.J., Zhang, X., Hendon, H.H., and Wheeler, M.C. (2006). Large scale dynamics and MJO forcing of ENSO variability. *Geophysical Research Letters* 33.

Mcwhorter, J.K., Halloran, P.R., Roff, G., Skirving, W.J., Perry, C.T., and Mumby, P.J. (2022). The importance of 1.5°C warming for the Great Barrier Reef. *Global Change Biology* 28**,** 1332-1341.

Min, S.-K., Cai, W., and Whetton, P. (2013). Influence of climate variability on seasonal extremes over Australia. *Journal of Geophysical Research: Atmospheres* 118**,** 643-654.

Mitchell, J.F.B., Lowe, J., Wood, R.A., and Vellinga, M. (2006). Extreme events due to human-induced climate change. *Philosophical Transactions of the Royal Society A: Mathematical, Physical and Engineering Sciences* 364**,** 2117-2133.

O'mahoney, J., Simes, R., Redhill, D., Heaton, K., Atkinson, C., Hayward, E., and Nguyen, M. (2017). "At what price? The economic, social and icon value of the Great Barrier Reef". Deloitte. Access Economics.).

Oke, P.R., Griffin, D.A., Schiller, A., Matear, R.J., Fiedler, R., Mansbridge, J., Lenton, A., Cahill, M., Chamberlain, M.A., and Ridgway, K. (2013). Evaluation of a near-global eddy-resolving ocean model. *Geosci. Model Dev.* 6**,** 591-615.

Osborne, K., Dolman, A.M., Burgess, S.C., and Johns, K.A. (2011). Disturbance and the dynamics of coral cover on the Great Barrier Reef (1995–2009). *PloS one* 6**,** e17516.

Philander, S.G.H. (1983). El Niño Southern Oscillation phenomena. *Nature* 302**,** 295-301.

Redondo-Rodriguez, A., Weeks, S.J., Berkelmans, R., Hoegh-Guldberg, O., and Lough, J.M. (2011). Climate variability of the Great Barrier Reef in relation to the tropical Pacific and El Nino-Southern Oscillation. *Marine and Freshwater Research* 63**,** 34-47.

Reynolds, R.W., Smith, T.M., Liu, C., Chelton, D.B., Casey, K.S., and Schlax, M.G. (2007). Daily high-resolution-blended analyses for sea surface temperature. *Journal of Climate* 20**,** 5473-5496.

Smith, G., and Spillman, C. (2019). New high-resolution sea surface temperature forecasts for coral reef management on the Great Barrier Reef. *Coral Reefs* 38**,** 1039-1056.

Sobel, A., Wang, S., and Kim, D. (2014). Moist static energy budget of the MJO during DYNAMO. *Journal of the Atmospheric Sciences* 71**,** 4276-4291.

Spillman, C.M., and Alves, O. (2009). Dynamical seasonal prediction of summer sea surface temperatures in the Great Barrier Reef. *Coral Reefs* 28**,** 197-206.

Sully, S., Burkepile, D.E., Donovan, M.K., Hodgson, G., and Van Woesik, R. (2019). A global analysis of coral bleaching over the past two decades. *Nature Communications* 10**,** 1264.

Trenberth, K.E., Fasullo, J.T., and Shepherd, T.G. (2015). Attribution of climate extreme events. *Nature Climate Change* 5**,** 725-730.

Wang, B., Chen, G., and Liu, F. (2019). Diversity of the Madden-Julian oscillation. *Science Advances* 5**,** eaax0220.

Wang, B., Wu, R., and Li, T. (2003). Atmosphere–Warm Ocean Interaction and Its Impacts on Asian–Australian Monsoon Variation. *Journal of Climate* 16**,** 1195-1211.

Wheeler, M.C., and Hendon, H.H. (2004). An all-season real-time multivariate MJO index: Development of an index for monitoring and prediction. *Monthly weather review* 132**,** 1917-1932.

Whiteman, H., Ritchie, H., and Regan, H. 2022. Great Barrier Reef suffers sixth mass bleaching event with 91% of reefs surveyed affected. Available: https://edition.cnn.com/2022/05/11/australia/australia-great-barrier-reef-bleaching-climate-intl-hnk/index.html.

Yee, S.H., and Barron, M.G. (2010). Predicting coral bleaching in response to environmental stressors using 8 years of global-scale data. *Environmental monitoring and assessment* 161**,** 423-438.

Zangvil, A. (1975). Temporal and spatial behavior of large-scale disturbances in tropical cloudiness deduced from satellite brightness data. *Mon. Wea. Rev.* 103**,** 904-920.

Zhang, C. (2005). Madden-julian oscillation. *Reviews of Geophysics* 43.

Zhang, C., and Gottschalck, J. (2002). SST anomalies of ENSO and the Madden–Julian oscillation in the equatorial Pacific. *Journal of Climate* 15**,** 2429-2445.

Zhao, W., Huang, Y., Siems, S., and Manton, M. (2021). The Role of Clouds in Coral Bleaching Events Over the Great Barrier Reef. *Geophysical Research Letters* 48**,** e2021GL093936.